



## A direct carbon fuel cell with (molten carbonate)/(doped ceria) composite electrolyte

Lijun Jia<sup>a,b</sup>, Ye Tian<sup>a,b</sup>, Qinghua Liu<sup>a,b</sup>, Chun Xia<sup>a,b</sup>, Jinshuai Yu<sup>a,b</sup>, Zhiming Wang<sup>a,b</sup>, Yicheng Zhao<sup>a,b</sup>, Yongdan Li<sup>a,b,\*</sup>

<sup>a</sup> Tianjin Key Laboratory of Catalysis Science and Technology, School of Chemical Engineering, Tianjin University, Tianjin 300072, China

<sup>b</sup> State Key Laboratory for Chemical Engineering, School of Chemical Engineering, Tianjin University, Tianjin 300072, China

### ARTICLE INFO

#### Article history:

Received 1 February 2010

Received in revised form 6 March 2010

Accepted 8 March 2010

Available online 12 March 2010

#### Keywords:

Direct carbon fuel cell

Carbon

Molten carbonate

Ceria

Composite electrolyte

### ABSTRACT

A composite electrolyte containing a Li/Na carbonate eutectic and a doped ceria phase is employed in a direct carbon fuel cell (DCFC). A four-layer pellet cell, viz. cathode current collector (silver powder), cathode (lithiated NiO/electrolyte), electrolyte and anode current collector layers (silver powder), is fabricated by a co-pressing and sintering technique. Activated carbon powder is mixed with the composite electrolyte and is retained in the anode cavity above the anode current collector. The performance of the single cell with variation of cathode gas and temperature is examined. With a suitable CO<sub>2</sub>/O<sub>2</sub> ratio of the cathode gas, an operating temperature of 700 °C, a power output of 100 mW cm<sup>-2</sup> at a current density of 200 mA cm<sup>-2</sup> is obtained. A mechanism of O<sup>2-</sup> and CO<sub>3</sub><sup>2-</sup> binary ionic conduction and the anode electrochemical process is discussed.

© 2010 Elsevier B.V. All rights reserved.

### 1. Introduction

Direct carbon fuel cell (DCFC) converts chemical energy of solid carbon fuel to electricity directly with a high efficiency [1–5]. Different from a hydrogen fuel cell, DCFC uses solid carbon directly as fuel. This brings several advantages. The theoretical thermal efficiency of DCFC is slightly over 100% due to the entropy change of the cell reaction given as Eq. (1) is slightly positive [2]:



Compared to hydrogen, carbon is more convenient for storage and transportation and is less fire/explosion hazard [6]. Finally, almost all the carbon-rich materials, such as coal, natural gas, petroleum, and biomass can be easily converted or purified to the fuel of DCFC [5–10].

Research effort has been focused on the design of DCFC devices and improvement of cell performance. According to the diversity of electrolyte, DCFC is classified into several categories [2]. Using molten carbonate as electrolyte, Cooper and co-workers [1,7,11–13] established several types of DCFC devices with carbon particulates anode fuel dispersed in molten carbonate electrolyte.

The effect of carbon structure was examined [1,7,11,14]. A good performance with a maximum power density of 100 mW cm<sup>-2</sup> at a current density of 120 mA cm<sup>-2</sup> was obtained when using a tilted orientation design and at an operating temperature of 800 °C [13]. Li and co-workers [10,15] proposed a DCFC anode kinetic model and a single cell model, besides, they also simulated the electrochemical processes in DCFC. Zecevic et al. [6] used a molten hydroxide electrolyte and a Fe–Ti alloy container, serving also as the cathode, and obtained an average power output of 40 mW cm<sup>-2</sup> at the maximum current density of 250 mA cm<sup>-2</sup>. Molten hydroxide, which was used as electrolyte in the early DCFC designs [4], have a high ionic conductivity and reactivity in the electrochemical oxidation of carbon, and facilitate a low temperature, e.g. 600 °C, operation of the DCFC device [6]. However, the stability of the cathode, i.e. the container, is a challenge. A solid oxide electrolyte in DCFC solves the depletion and corrosion problems of the molten electrolyte [16]. Tao [17] constructed a DCFC using (ZrO<sub>2</sub>)(HfO<sub>2</sub>)<sub>0.02</sub>(Y<sub>2</sub>O<sub>3</sub>)<sub>0.08</sub> as the electrolyte and obtained a power output of 10 mW cm<sup>-2</sup> at 0.248 V at 800 °C and 50 mW cm<sup>-2</sup> at 0.507 V at 1002 °C, respectively. Recently, Irvine and co-workers [8,18] fed a mixed carbonate and carbon fuel into the anode compartment and used yttria stabilized zirconia (YSZ) as the electrolyte. With this design, a high open circuit potential (OCP) of about 1.5 V and the maximum power density of 13 mW cm<sup>-2</sup> at 900 °C was achieved [19]. Obviously, DCFC using solid oxide electrolyte needs a high temperature to achieve enough ionic conductivity, which may lead to formation of CO due to Boudouard reaction [20]. On the other hand, the electrochemical

\* Corresponding author at: Tianjin Key Laboratory of Catalysis Science and Technology, School of Chemical Engineering, Tianjin University, Weijin Road 92, Tianjin 300072, China. Tel.: +86 22 27405613; fax: +86 22 27405243.

E-mail address: [ydli@tju.edu.cn](mailto:ydli@tju.edu.cn) (Y. Li).

**Table 1**  
The ions conducted and the electrochemical reactions happened in DCFCs with different electrolytes.

Electrolyte	Conductive ions	Anode reaction	Cathode reaction	Overall reaction
Molten carbonate	$\text{CO}_3^{2-}$	$\text{C} + 2\text{CO}_3^{2-} \rightarrow 3\text{CO}_2 + 4\text{e}^-$	$\text{O}_2 + 2\text{CO}_2 + 4\text{e}^- \rightarrow 2\text{CO}_3^{2-}$	$\text{C} + \text{O}_2 \rightarrow \text{CO}_2$
Molten hydroxide	$\text{OH}^-$	$\text{C} + 4\text{OH}^- \rightarrow \text{CO}_2 + 2\text{H}_2\text{O} + 4\text{e}^-$	$\text{O}_2 + 2\text{H}_2\text{O} + 4\text{e}^- \rightarrow 4\text{OH}^-$	$\text{C} + \text{O}_2 \rightarrow \text{CO}_2$
Solid oxide	$\text{O}^{2-}$	$\text{C} + 2\text{O}^{2-} \rightarrow \text{CO}_2 + 4\text{e}^-$	$\text{O}_2 + 4\text{e}^- \rightarrow 2\text{O}^{2-}$	$\text{C} + \text{O}_2 \rightarrow \text{CO}_2$

reaction of solid carbon fuel is restricted by the contact between the fuel and the electrolyte; a high over-potential appears as a result [2].

Table 1 lists the major conductive ions, electrode semi-reactions and overall cell reactions with the three kinds of electrolytes used in DCFC [1–10]. For instance, carbonate ion is the major ion conducted in molten carbonate as the electrolyte [5,7]. Therefore, two molecules of carbon dioxide are required for the reduction of each oxygen molecule into carbonate phase in cathode compartment. At the same time, each carbon atom is oxidized by two carbonate ions with releasing of three carbon dioxide molecules and discharging of four electrons at the anode. One of the common features of the three kinds of electrolytes for DCFC is that each of them just conducts one kind of ion. Nevertheless, the overall cell reaction is the same as that each carbon atom is oxidized into carbon dioxide with consuming one molecular oxygen.

A solid composite electrolyte composed of a molten salt phase, such as mixed hydroxides or carbonates, and an oxygen ion conducting porous solid phase, such as samarium doped ceria (SDC) has been used in solid oxide fuel cells (SOFCs) [16,21–25]. The conductivity of this kind of composite electrolyte in an intermediate temperature (IT, 400–700 °C) range is much higher than the conventional solid electrolyte used in SOFC [26] and the molten electrolyte in molten carbonate fuel cell (MCFC). The high conductivity of the composite electrolyte has been explained by the enhancing effect of the ionic conduction in the two phases [27,28]. The composite electrolyte can be fabricated easily into a certain shape to support the cell structure. The SOFC constructed with the composite electrolyte has shown remarkably good cell performance [16,29].

In this work, a composite electrolyte composed of a molten carbonate and a porous SDC phase is examined. Based on this electrolyte, a DCFC device is fabricated and measured. The performance of the fuel cell and the ionic conduction mechanism is discussed.

## 2. Experimental

### 2.1. Preparation of cell materials

Binary carbonate eutectic powder, i.e.  $\text{Li}_2\text{CO}_3/\text{Na}_2\text{CO}_3$  in a mole ratio of 2:1, was prepared by a process of sequential ball milling for 4 h, co-sintering at 700 °C for 2 h and grinding. An oxalate coprecipitation technique was chosen to prepare the SDC powder [25]. Composite electrolyte material powder was obtained through mixing the two powders in a weight ratio of 3:7 by ball milling for 4 h. Lithiated NiO was prepared through a solid-state reaction, during which the mixture of LiOH and NiO in a mole ratio of 1:1 was co-sintered at 700 °C for 2 h [21]. The composite cathode powder, which consists of 30 wt% the composite electrolyte and 70 wt% the lithiated NiO powders, was also prepared through 4 h ball mill mixing, sintering at 700 °C for 2 h and grinding process.

### 2.2. DCFC single cell design

A schematic diagram of the DCFC single cell is presented in Fig. 1, which contains several parts, two main compartments, i.e. anode and cathode cavities, and a four-layer cell pellet and a stainless steel container with inlets and outlets. The green four-layer pellet was

fabricated by a uniaxial co-pressing technique [16], during which different kinds of powders, i.e. silver (cathode current collector), composite cathode, composite electrolyte and silver (anode current collector) were fed into the die layer by layer with the aid of a 60 mesh sieve and pressed into a cylindrical pellet at 500 MPa with a diameter of 13 mm and thickness of 1 mm (mainly containing electrolyte 0.65 mm, cathode 0.35 mm). After sintering at 700 °C for 2 h, the cell pellet was sealed in the reactor with the cathode downwards. A stainless steel ring above the cell pellet, viz. anode cavity, was used to retain the mixture of activated carbon fuel and the binary molten carbonate salt at a weight ratio of 1:9. The stainless steel components, supporting the whole structure, were used as both the electrode and the gas distributor.

### 2.3. Characterization of DCFC materials

All the fuel cell materials were characterized with X-ray diffraction (XRD) at room temperature using a D/max 2500 v/pc instrument (Rigaku Corp., Japan) with  $\text{CuK}\alpha$  radiation. The morphology of both the four-layer cell pellet and the powders were examined with a Hitachi S-4800 scanning electron microscope (SEM).

### 2.4. Fuel cell performance test

The current–voltage ( $I$ – $V$ ) and the current–power ( $I$ – $P$ ) values were collected based on the four-terminal configuration using an electronic load, SM-102, made by Sanmusen Corp. in China. The fuel cell was tested in a working temperature range of 600–750 °C under atmospheric pressure. Anode protective gas nitrogen and different cathode gases:  $\text{CO}_2/\text{O}_2$  at mole ratios 2:1,  $\text{CO}_2/\text{O}_2$  at mole ratios 1:1, air and pure  $\text{O}_2$  were adopted at a gas flow rate of  $100 \text{ ml min}^{-1}$  (STP) in both sides. The measurements of OCP–temperature relationship started from 30 °C to 700 °C with a heating-rate of  $10 \text{ }^\circ\text{C min}^{-1}$ , then holded the temperature at 700 °C

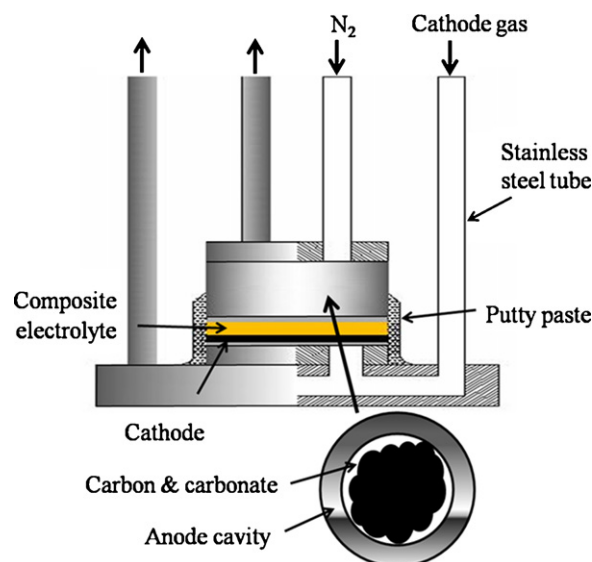


Fig. 1. The schematic diagram of the DCFC single cell.

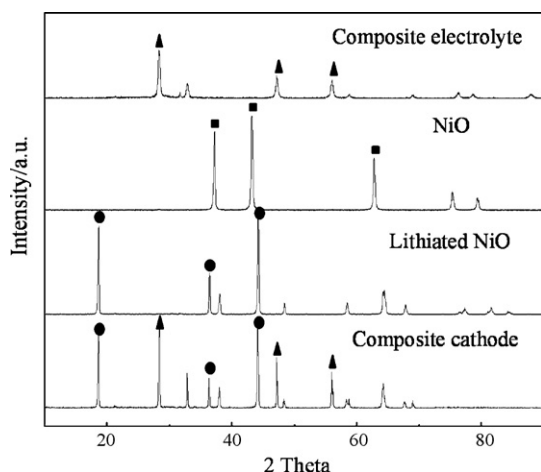


Fig. 2. The XRD patterns of the materials used.

for about 9 h and collected the OCP values at every 0.1 s using an electrochemical workstation, CHI660B, made by Cheng Hua Corp in China. During this measurement, anode protective nitrogen gas ( $100 \text{ ml min}^{-1}$ ) was started from  $450^\circ\text{C}$  and cathode gas ( $\text{CO}_2/\text{O}_2$  at mole ratios of 1:1,  $100 \text{ ml min}^{-1}$ ) was started when the temperature reached  $700^\circ\text{C}$ .

### 3. Results and discussion

#### 3.1. Properties of the cell materials

Fig. 2 shows the XRD patterns of the electrolyte and cathode powder. The composite electrolyte shows only the pattern of the cubic fluorite structure same as pure SDC phase [22]. No peaks belong to the carbonate phase appear indicating that the carbonate eutectic in the composite electrolyte exists as an amorphous phase, which was observed in the previous work [23]. The average

crystallite size of SDC particles in the composite electrolyte is 21 nm calculated according to the Scherrer formula  $D = 0.9\lambda / \beta \cos \theta$ , where  $\beta$  is obtained from the formula of  $\beta = (\beta_m^2 - \beta_s^2)^{1/2}$  [22]. Apparently, lithiated NiO and SDC are the major phases in the pattern of the composite cathode material. We can also conclude that there is no solid reaction between the carbonate and the lithiated NiO according to the patterns presented in Fig. 2.

The SEM micrographs of the materials used in the DCFC single cell are shown in Fig. 3. Differing from the pure SDC in previous reports [16,24] where it shows a rod-like appearance, the SDC in the composite at room temperature appears as small spherical domains coated by amorphous carbonate eutectic uniformly as Fig. 3(a). The secondary SDC aggregates are also quite homogeneous with an average size of around 80 nm. The above-mentioned difference in morphology of SDC phase may be due to a prolonged ball milling process employed in this work. The SEM graphs of the surface and the cross-section of the pellet are shown as Fig. 3(b) and (c), respectively. In these two micrographs, it is difficult to distinguish SDC particles from the carbonate phase because the SDC particles are coated completely by the solidified carbonate which once melted. Cracks and pores are clearly seen in the cross-section of Fig. 3(c), although it looks like a dense layer in the surface micrograph (Fig. 3(b)) at room temperature. However, during the operation above the melting temperature of the carbonate eutectic, the pores and cracks in the electrolyte layer will be fully filled with the molten carbonate, preventing the cathode gas leaking through, which is proved by the high open circuit potential (OCP)  $> 1.0 \text{ V}$  measured in this work. This agrees with the previous results [16]. As shown in Fig. 3(d), the electrolyte particles and lithiated NiO particles are mixed thoroughly in the cathode material and these two phases can be distinguished in the graph easily because of different structure and size. The verification with EDAX tells also that the larger particles are lithiated NiO and the smaller ones are the SDC phase. The SEM micrograph also reconfirms that both the two phases exist simultaneously without any reaction. Both SDC and lithiated NiO have a trend of aggregation after pressing them into pellet. However, the interfaces between the SDC and the lithiated

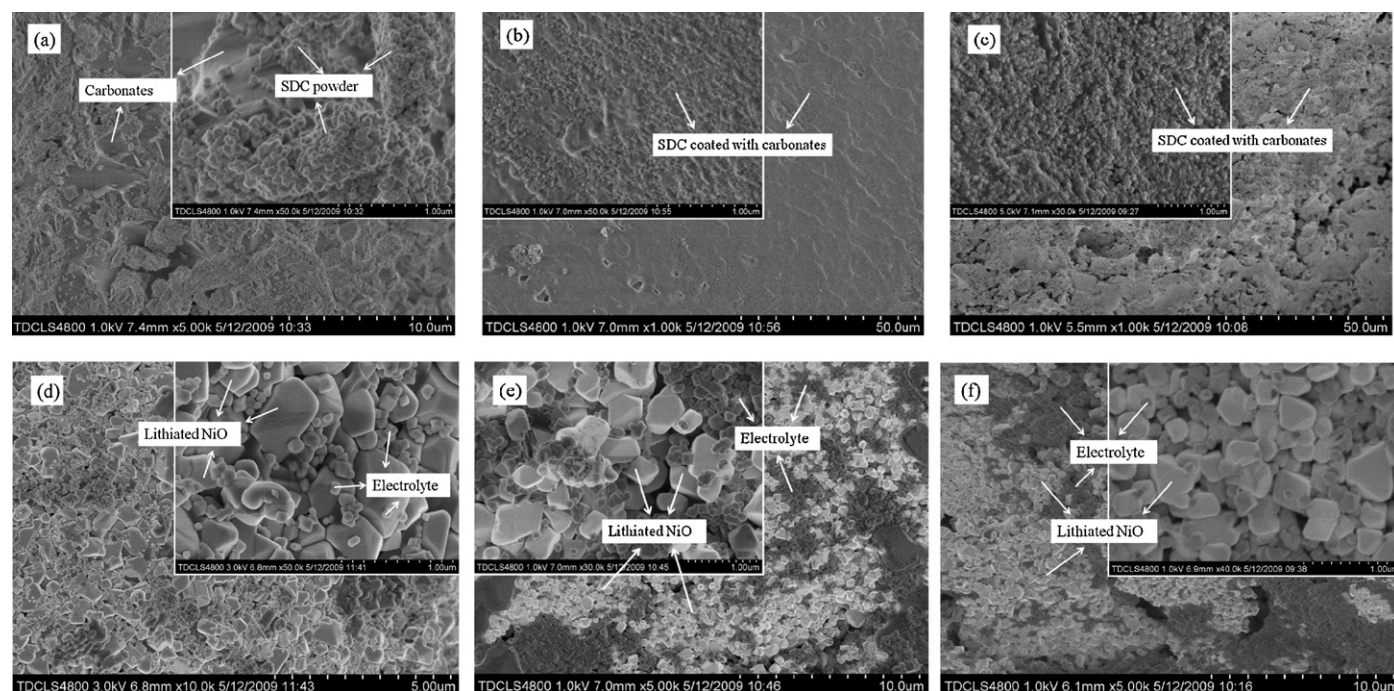


Fig. 3. The SEM micrographs of the materials used. (a) Composite electrolyte powder, (b) the surface views, (c) cross-sectional views of electrolyte side of the pellet, (d) cathode powder, (e) the surface views, and (f) cross-sectional views of the cathode side of the pellet.

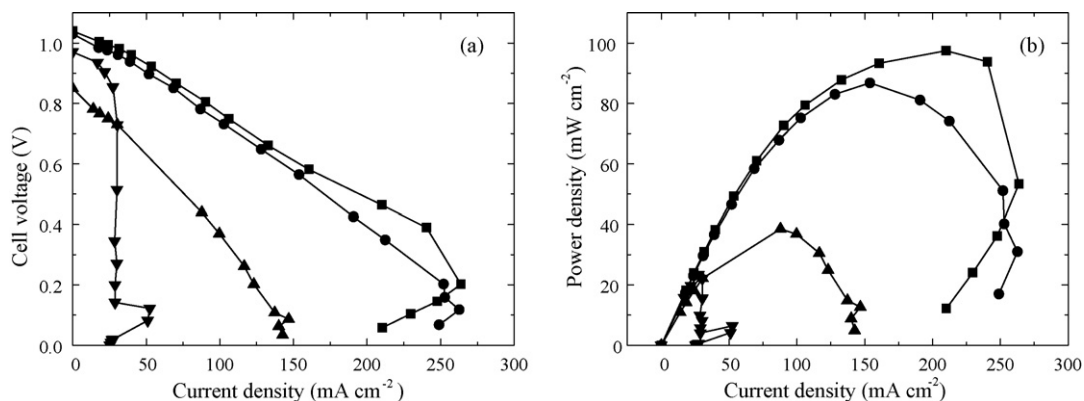


Fig. 4. The  $I$ - $V$  (a) and  $I$ - $P$  (b) curves with different cathode gases measured at 700 °C. (■)  $\text{CO}_2/\text{O}_2$  2:1, (●)  $\text{CO}_2/\text{O}_2$  1:1, (▲) air, and (▼)  $\text{O}_2$ .

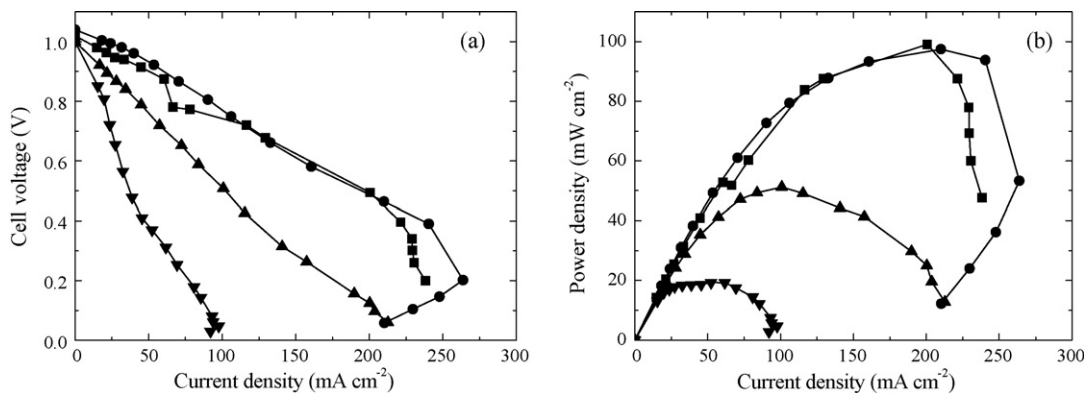


Fig. 5. The  $I$ - $V$  (a) and  $I$ - $P$  (b) curves at different operating temperatures. (■) at 750 °C, (●) at 700 °C, (▲) at 650 °C, and (▼) at 600 °C.

NiO phases in both the surface and the cross-section images are still clear as shown in Fig. 3(e) and (f). Pores with different size and shape exist in the cathode pellet, and the triple phase boundary (TPB) forms significantly due to the addition of the electrolyte material to the cathode. The composite cathode material enhances both the active zone and the interface for the electrochemical reaction which contributes also to the ionic conduction rate.

### 3.2. Performance of DCFC single cell

Fig. 4(a) and (b) depicts the  $I$ - $V$  and  $I$ - $P$  curves at 700 °C with different cathode gases. The OCPs of the single cell are 1.04 V, 1.03 V, 0.84 V and 0.97 V with  $\text{CO}_2/\text{O}_2$  2:1,  $\text{CO}_2/\text{O}_2$  1:1, air and pure  $\text{O}_2$  as cathode gases, respectively. When pure  $\text{O}_2$  was used as the cathode gas, the maximum current density of  $50 \text{ mA cm}^{-2}$  was achieved and cannot be increased further.  $\text{O}^{2-}$  is considered as the dominant conductive ion when using  $\text{O}_2$  as the cathode gas, so that the conductivity of the electrolyte is limited. The cell performance is enhanced significantly when  $\text{CO}_2$  is added into the cathode gas. As a consequence, the power density approached or stepped over  $100 \text{ mW cm}^{-2}$  when the  $\text{CO}_2/\text{O}_2$  mixtures are used as the cathode gas. The  $I$ - $V$  and  $I$ - $P$  curves at different operating temperatures in a range of 600–750 °C are plotted in Fig. 5(a) and (b). The performance of the cell is enhanced significantly with the increase of temperature from 600 °C to 700 °C. This may be correlated to a decrease in viscosity of the molten carbonate phase and an enhancement of the ionic conduction rate in the electrolyte and the electrochemical reactions of both electrodes [30]. An interesting phenomenon is noticed that the curves rounded back at high current densities, which is probably due to the over consumption of carbon fuel in anode compartment and the formation of gaps for the contact of the

fuel and the electrolyte layers. These curves were recorded starting from the low current density end. Another measurement of cell performance was also exerted by starting from the high current density end, i.e. low voltage end. In that case the curving back phenomenon was not observed, it is a reconfirmation of the above explanation.

Fig. 6 represents the changes of OCP with the operating temperature and time. Three points should be noticed. At point A, i.e. 500 °C, a sharp increase of the OCP is observed due to the ionic conduction in the molten carbonate phase and the melting of the salts, here 497 °C. The switch to  $\text{CO}_2/\text{O}_2$  cathode gas leads to another increase, i.e. pointed B. After that, the OCP decreases due to an aging process of the electrochemical reaction, which results in a stable OCP at 1.04 V for quite a while. However, the high OCP close to the theo-

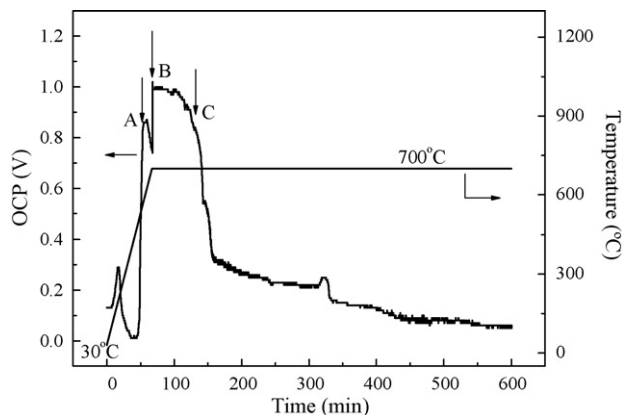


Fig. 6. OCP-time and temperature curve of the DCFC in this work.

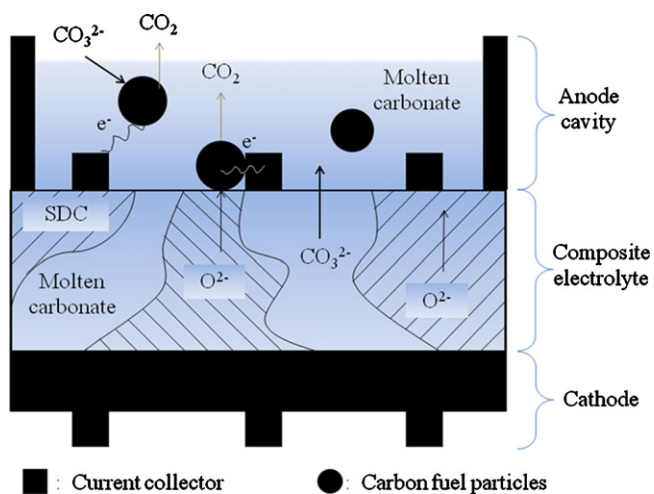


Fig. 7. Scheme of the electrochemical process in a DCFC single cell.

retical value drops suddenly at point C after 2 h fairly stable period. The OCP decline after point C is due to the carbon consumption. While the research on the improvement of the stability is ongoing, the results presented here is useful only for understanding the initial stage of the fuel cell reaction.

### 3.3. Mechanisms

#### 3.3.1. Ionic conduction in electrolyte

Here, a working model of a DCFC illustrating the ionic conduction and reactions in the electrolyte and electrode are presented in Fig. 7. In the previous works on SOFCs with a composite electrolyte, multi-ionic conduction in the composite electrolyte has been assumed [16,26]. In this work, the carbonate in both the electrolyte and the anode cavity is in melting state. Therefore, no leak of gases through the electrolyte happens due to the fact that the pores and cracks in SDC phase are filled and wetted with molten carbonate. The carbon particles in the anode cavity are also wetted by the molten carbonate. When cathode gas is the mixture of  $O_2/CO_2$ , both  $O^{2-}$  ions and  $CO_3^{2-}$  ions transfer happens in the composite electrolyte and are electrical conductive.  $O^{2-}$  ions are conducted along the SDC bulk phase while  $CO_3^{2-}$  ions transfer through the molten carbonate phase [16]. Li et al. [27] and Rui et al. [28] proposed that the overall conductivity of the composite electrolyte composed of an  $O^{2-}$  conductive porous phase such as SDC and a  $CO_3^{2-}$  conductive molten carbonate phase is much higher than both the two phases when functioned individually. The  $O^{2-}$  conduction and  $CO_3^{2-}$  conduction enhances each other in the composite electrolyte due to the following reaction happens at the interface close to the cathode:



#### 3.3.2. Electrode reactions

In the conventional DCFC using carbonate as electrolyte, the molten carbonate is retained in a porous insulator by capillary force and  $CO_3^{2-}$  is the major conductive ion [16]. The reactivity between  $CO_3^{2-}$  and carbon fuel is acceptable because sometimes high output power density around  $100 \text{ mW cm}^{-2}$  was achieved [7]. In another work on DCFC, solid oxide electrolyte conducting  $O^{2-}$  ions were used and an overall output power of 50 mW was obtained [31]. In this work, SDC phase is an  $O^{2-}$  conductor and the molten carbonate phase is a  $CO_3^{2-}$  conductor. Both  $CO_3^{2-}$  and  $O^{2-}$  ions are conducted simultaneously when using  $CO_2/O_2$  mixture as the cathode gas, which also leads to complicated electrode reactions. In anode compartment, the carbon particles contacting with the

solid oxide electrolyte react with  $O^{2-}$  ions to produce carbon dioxide and release electrons, whereas the carbon particles dispersing in the molten carbonate phase directly react with  $CO_3^{2-}$  ion and produces carbon dioxide and electrons simultaneously. In cathode compartment, the oxygen atom can be directly reduced into oxygen ions and also react with  $CO_2$  to generate carbonate ions. The anode and cathode reactions can be expressed as:

Anode reaction:



Cathode reaction:



Haupin and Frank [32] proposed a mechanism for the anode reaction which was called Hall process later [7] and was adopted by Cooper et al. [7] to describe the process in which carbon reacts only with  $O^{2-}$ . The carbon atom at a reactive site is attacked by  $O^{2-}$  leading to a discharge of two electrons. The first  $O^{2-}$  forms a C–O–C bridge through several steps of interactions. The second  $O^{2-}$  adsorbed inserts to the next C–C bond and forms a C–O–C–O–C structure with releasing another two charges. Then  $CO_2$  is generated by cutting of the two C–O bonds [32]. However, it was reported that  $O^{2-}$  can be dissolved up to 0.5 mol% in a Li–Na–K ternary eutectic carbonate [33]. The anode electrochemical reaction may be restrained by the low  $O^{2-}$  concentration, resulting in a high anode polarization loss and a low power output. Nabaie et al. [19] proposed that  $CO_3^{2-}$  ion can oxidize carbon to  $CO_2$  directly. This increases the reaction zone and enhances the electrochemical oxidation of carbon. The concentration of  $CO_3^{2-}$  ion is high in the system.

Actually, many oxygen containing ions exist simultaneously in the molten electrolyte phase, such as  $O^{2-}$ ,  $CO_4^{2-}$ , and  $C_2O_6^{2-}$ . and may take part in the anode reaction [34]. The detailed anode reaction mechanism needs further elucidation.

## 4. Conclusions

A novel direct carbon single cell based on a Li/Na<sub>2</sub>CO<sub>3</sub>-samarium doped ceria composite electrolyte has been established and examined. The single cell employed a four-layer pellet as the main component, which contained cathode, electrolyte and current collector and was fabricated by a co-pressing technique. The cathode composite of lithiated NiO and the electrolyte material. Activated carbon, used as the anode fuel, is mixed with composite electrolyte and retained above on the electrolyte layer in the anode cavity. Using  $CO_2/O_2$  as the cathode gas improves the cell performance dramatically, which is attributed to the enhancement of the ionic conductivity in the electrolyte. A suitable working temperature is also beneficial to the cell performance. The maximum power density of  $100 \text{ mW cm}^{-2}$  at a current density of  $200 \text{ mA cm}^{-2}$  is obtained with the  $CO_2/O_2$  mixture as the cathode gas at temperature of  $700^\circ\text{C}$ . A binary ionic conduction and anode electrochemical reaction mechanism is proposed.

## Acknowledgements

This work has been supported by the Natural Science Foundation of China under contract numbers 20425619 and 20736007. The work has been also supported by the Program of Introducing Talents to the University Disciplines under file number B06006, and the Program for Changjiang Scholars and Innovative Research Teams in Universities under file number IRT 0641.

## References

- [1] J.F. Cooper, S&TR June (2001) 4.
- [2] D.X. Cao, Y. Sun, G.L. Wang, J. Power Sources 167 (2007) 250–257.
- [3] T.A. Edison, US Patent 460,122 (1891).
- [4] W.W. Jacques, US Patent 555,511 (1896).
- [5] X. Li, Z.H. Zhu, J.L. Chen, R.D. Marco, A. Dicks, J. Power Sources 186 (2009) 1–9.
- [6] S. Zecevic, E.M. Patton, P. Parhami, Carbon 42 (2004) 1983–1993.
- [7] N.J. Cherepy, R. Krueger, K.J. Fiet, A.F. Jankowski, J.F. Cooper, J. Electrochem. Soc. 152 (2005) A80–A87.
- [8] Y. Nabae, K.D. Pointon, J.T.S. Irvine, J. Electrochem. Soc. 156 (2009) B716–B720.
- [9] G.A. Hackett, J.W. Zondlo, R. Svensson, J. Power Sources 168 (2007) 111–118.
- [10] Q.H. Liu, Y. Tian, C. Xia, L.T. Thompson, B. Liang, Y.D. Li, J. Power Sources 185 (2008) 1022–1029.
- [11] J.F. Cooper, N. Cherepy, R.L. Krueger, US Patent 6,878,479 (2005).
- [12] J.F. Cooper, Design, efficiency and materials for carbon/air fuel cells, Presented in Direct Carbon Fuel Cell Workshop, NETL, Pittsburg, PA, USA, 30th July, 2003.
- [13] J.F. Cooper, Design, reactions of the carbon anode in molten carbonate electrolyte, Presented in Direct Carbon Fuel Cell Workshop, NETL, Pittsburg, PA, USA, 30th July, 2003.
- [14] J.L. Chen, X. Yang, Y.D. Li, Fuel 89 (2010) 943–948.
- [15] H.J. Li, Q.H. Liu, Y.D. Li, Electrochim. Acta 55 (2010) 1958–1965.
- [16] C. Xia, Y. Li, Y. Tian, Q.H. Liu, Y.C. Zhao, L.J. Jia, Y.D. Li, J. Power Sources 188 (2009) 156–162.
- [17] T. Tao, US Patent 6,692,861 (2004).
- [18] S.L. Jain, J.B. Lakeman, K.D. Pointon, J.T.S. Irvine, J. Fuel Cell Sci. Technol. 4 (2007) 280–282.
- [19] Y. Nabae, K.D. Pointon, J.T.S. Irvine, Energy Environ. Sci. 1 (2008) 148–155.
- [20] T.M. Gur, R.A. Huggins, J. Electrochem. Soc. 139 (1992) L95–L97.
- [21] J.B. Huang, L.Z. Yang, R.F. Gao, Z.Q. Mao, C. Wang, Electrochem. Commun. 8 (2006) 785–789.
- [22] K. Singh, S.A. Acharya, S.S. Bhoga, Ionics 13 (2007) 429–434.
- [23] A. Boden, J. Di, C. Lagergren, G. Lindbergh, C.Y. Wang, J. Power Sources 172 (2007) 520–529.
- [24] J.B. Huang, Z.Q. Mao, L.Z. Yang, Electrochem. Solid-State Lett. 8 (2005) A437–A440.
- [25] B. Zhu, X.T. Yang, J. Xu, Z.G. Zhu, J. Power Sources 118 (2003) 47–53.
- [26] B. Zhu, J. Power Sources 114 (2003) 1–9.
- [27] Y.D. Li, Z.B. Rui, C. Xia, M. Anderson, Y.S. Lin, Catal. Today 148 (2009) 303–309.
- [28] Z.B. Rui, M. Anderson, Y.S. Lin, Y.D. Li, J. Membr. Sci. 345 (2009) 110–118.
- [29] C. Xia, Y. Li, Y. Tian, Q.H. Liu, Z.M. Wang, L.J. Jia, Y.C. Zhao, Y.D. Li, J. Power Sources 195 (2010) 3149–3154.
- [30] S.L. Jain, Y. Nabae, B.J. Lakeman, K.D. Pointon, J.T.S. Irvine, Solid State Ionics 179 (2008) 1417–1421.
- [31] S.L. Jain, J.B. Lakeman, K.D. Pointon, R. Marshall, J.T.S. Irvine, Energy Environ. Sci. 2 (2009) 687–693.
- [32] W.B. Frank, W.E. Haupin, Ullmann's Encyclopedia of Industrial Chemistry, vol. A1, 5th ed., VCH, Deerfield Beach, FL, USA, 1985.
- [33] S. White, U. Twardoch, J. Appl. Electrochem. 19 (1989) 901–910.
- [34] G.B. Dunks, Inorg. Chem. 23 (1984) 828–837.